Modeling the nonequilibrium effects in a nonquasi-equilibrium thermodynamic cycle based on steepest entropy ascent and an isothermal-isobaric ensemble

Guanchen Li[*], Michael R. von Spakovsky

Center for Energy Systems Research, Mechanical Engineering Department, Virginia Tech, Blacksburg, VA 24061, USA

ABSTRACT

Conventional first principle approaches for studying nonequilibrium or far-from-equilibrium processes depend on the mechanics of individual particles or quantum states. They also require many details of the mechanical features of a system to arrive at a macroscopic property. In contrast, thermodynamics provides an approach for determining macroscopic property values without going into these details, because the overall effect of particle dynamics results, for example, at stable equilibrium in an invariant pattern of the "Maxwellian distribution", which in turn leads to macroscopic properties. However, such an approach is not generally applicable to a nonequilibrium process except in the near-equilibrium realm. To adequately address these drawbacks, steepest-entropy-ascent quantum thermodynamics (SEAQT) provides a first principle, thermodynamic-ensemble approach applicable to the entire nonequilibrium realm. Based on prior developments by the authors, this paper applies the SEAQT framework to modeling the nonquasi-equilibrium cycle, which a system with variable volume undergoes. Using the concept of hypoequilibrium state and nonequilibrium intensive properties, this framework provides a complete description of the nonequilibrium evolution in state of the system. Results presented here reveal how nonequilibrium effects influence the performance of the cycle.

© 2016 Elsevier Ltd. All rights reserved.

1. Introduction

Numerous methods for modeling nonequilibrium phenomena exist with each restricted to its own applicable set of spatial and temporal scales. At the macroscopic level, continuum nonequilibrium thermodynamics with the local equilibrium assumption is used but cannot generally be applied at atomistic/mesoscopic levels since the small dimensions of a system result in quantum and for that matter classical effects that the continuum assumption cannot address. Furthermore, nonequilibrium processes in the far-from-equilibrium realm make the application of the continuum formulation of nonequilibrium thermodynamics, i.e., the so-called Onsager formulation (e.g., [1]) questionable due to its underlying assumption of linearity or near-equilibrium behavior. In addition, each method uses a different kinematic and dynamic description of

system state and its motion. Thus, a general approach that provides a thermodynamic analysis of nonequilibrium evolution, especially that far-from-equilibrium, across different spatial and temporal scales has been lacking even though general system properties such as the energy and entropy are well defined [2] and their evolutions observable. Steepest-entropy-ascent quantum thermodynamics (SEAQT) [3–11] addresses these issues providing a mathematical framework with a single kinematics and dynamics that crosses all temporal and spatial scales and accounts for both non-continuum quantum and classical effects. At the same time, it is able to provide system property information based on a fundamental as opposed to phenomenological description and thermodynamic system features resulting from nonequilibrium relaxation patterns (in the sense of GENERIC [12,13]), which capture the dynamic balance of detailed and complex microscopic single particle or quantum state evolutions. These patterns represent a reduction of a system's microscopic kinematics, appear to be general, and are independent of the microscopic dynamics, i.e., of the exact form of the micro-mechanical interactions. One of the benefits of this is that the SEAQT framework is able to avoid the computational burdens inherent to existing methods based on mechanics (e.g., the

Boltzmann equation [14—16] and molecular dynamics [17]) or quantum mechanics (e.g., 'open-system' quantum thermodynamics [18—23], 'closed quantum systems' [24], heat reservoirs mediated by quantum systems [25], quantum nonequilibrium Green's function equations of motion [26—28], and the quantum Boltzmann equation, i.e., the Uehling-Uhlenbeck-Boltzmann equation [29—31]) that require detailed interaction information of the particles or quantum states.

To date, SEAQT has successfully been used to model nonequilibrium processes (even those far-from equilibrium) from the atomistic to the macroscopic level [9—11,32—37] and bases its framework on properties such as energy, particle number, and entropy, which as mentioned before, are well-defined at all scales for equilibrium as well as nonequilibrium states [2]. The non-linear dynamics of state evolution are characterized by the entropy generation, which results from the principle of steepest entropy ascent (or maximum entropy production [38]). This principle forms the basis of the equation of motion that tracks the evolution of energy and entropy in state space. Using the concept of hypoequilibrium state [9] (i.e., a nonequilibrium relaxation pattern), the nonequilibrium trajectory of system state evolution can be fully described across a wide range of initial conditions. In this way, the thermodynamic analysis of nonequilibrium phenomena at different scales, whether classical or quantum, can be studied using a single framework, i.e., a single kinematics and dynamics.

Since an important part of thermodynamics is to study systems for which volume is the only parameter (in the sense of Gyftopolous and Beretta [39,40]), a description of such a system undergoing a cyclic process in the nonequilibrium realm using SEAQT is presented here. Clearly, an important application of thermodynamics is to the study of such processes independent of the exact nature of the microscopic interactions, which take place inside the system. Cyclic processes have been modeled both at the macroscopic level using equilibrium thermodynamics as well as at the quantum level using quantum mechanics [41—43]. The limitation with respect to the former is that the study of a cycle for such a system necessarily assumes that the system (e.g., that of a gas in a piston/cylinder device) is in a stable equilibrium state at any given instant of time and undergoes a quasi-equilibrium process, i.e., the state evolution of the system is very, very slow and the process is reversible. To move the analysis into the practical realm requires the introduction of phenomenological parameters (e.g., experimental polytropic exponents, isentropic efficiencies) to help account for the effects of irreversibilities and, thus, model real engine cycles and guide device design. The limitation with respect to the latter, i.e., approaches based solely on quantum mechanics (e.g., 'open quantum systems' [41,42]), is that the thermodynamic laws appear only to emerge from the results of the quantum master equation of a given approach but are not fundamental to it and are, thus, only used to validate the model set-up [44,8]. Such approaches can provide insight into the mechanical basis of thermodynamics for a limited set of very specific conditions (e.g., weak system-environment interactions or steady state) but predicting all the general effects, which result directly from the laws of thermodynamics is very difficult and may in fact be impossible when, the mechanical interaction details are too complex or simply not available. Thus, the application of such approaches focuses on quantum systems in nonequilibrium but in general cannot be extended to the modeling of classical meso/macroscopic systems in nonequilibrium states, especially those in the far-from-equilibrium realm. In contrast, the SEAQT framework provides a single theoretical model of irreversibility at all temporal and spatial scales based on the laws of thermodynamics, i.e., they are fundamental to the description. The use of the concept of density of states [32,9] with this framework permits tracking the time evolution of all the energy eigenlevels of

a system and does so at a relatively small computational expense, enabling the application of this framework to a wide range of systems at the micro/meso/macro levels using energy eigenlevel information developed from experimental measurements or the computational results of quantum chemistry or density functional theory. In addition, using the concept of hypoequilibrium state and rigorous definitions of nonequilibrium intensive properties [9,10], greater physical insight into the influence of nonequilibrium effects on system performance can be revealed.

In the following, unique thermodynamic trajectories for system state evolutions from some initial transient state to steady state are predicted for cyclic processes using the SEAQT equation of motion. This equation is derived from the conservation laws and the principle of steepest-entropy-ascent (or maximum-entropy-production), i.e., from the first and second laws of thermodynamics, and is introduced and discussed in Sections 2.1—2.3 along with the system and state space considered and the quantum and classical system descriptions used. The concepts of hypoequilibrium state, temperature, and pressure for nonequilibrium states are introduced in Section 2.4 and are shown to be closely related to the isothermal-isobaric ensemble of stable equilibrium [45—49]. The definitions of temperature and pressure proposed for nonequilibrium states are fundamental rather than phenomenological and a generalization of these properties from those at stable equilibrium. The SEAQT equation of motion for two interacting systems and for a system interacting with a reservoir are then presented in Section 3 followed in Section 4 by a description of a system undergoing a nonquasi-equilibrium evolution in state. These examples illustrate the inputs and outputs of the model. Finally, in Section 5, results are given for the state time evolution of a system undergoing a transient cyclic process. How nonequilibrium phenomena influence the performance of the cycle is discussed, and a simple case of optimizing the power of the cyclic system relative to the nonequilibrium effects is illustrated.

2. SEAQT equation of motion

2.1. SEAQT equation of motion using a quantum mechanical description

In this section, the system and state description in SEAQT used here is given, and the equation of motion presented. Based on the discussion by Grmela and Öttinger [12,13,50] and Beretta et al. [7,51] the general form of a nonequilibrium framework is a combination of both irreversible relaxation and reversible symplectic dynamics. If written in the generalized form of the Ginzburg-Landau equation [12,51], the equation of motion takes the following form:

$$\frac{d}{dt}\gamma(t) = X^H_{\gamma(t)} + Y^H_{\gamma(t)} \tag{1}$$

where $\gamma(t)$ represents the state evolution trajectory and $X^H_{\gamma(t)}$ and $Y^H_{\gamma(t)}$ are functions of the system state $\gamma(t)$ and represent the reversible symplectic and irreversible relaxation dynamics, respectively. In the SEAQT framework, the system is defined by the Hamiltonian operator $\widehat{H}$, system state is represented by the density operator $\widehat{\rho}$, $X^H_{\gamma(t)}$ follows the Schrödinger equation, and $Y^H_{\gamma(t)}$ is derived from the SEA principle. To describe the evolutionary process, conservation laws are explicitly required in order to construct the equation of motion, which is given in Ref. [52] as

$$\frac{d\widehat{\rho}}{dt} = \frac{1}{i\hbar}\left[\widehat{\rho}, \widehat{H}\right] + \frac{1}{\tau}\widehat{D} \tag{2}$$

where the first term is the Schrödinger term and the second the dissipation term. Two types of initial conditions can cause one term on the right hand side of the equation of motion to vanish. The first is that if the system is in a pure (zero-entropy) state initially, i.e., $\hat{\rho}\hat{\rho} = \hat{\rho}$, the equation of motion reverts back to the Schrödinger equation of quantum mechanics. The second is that if the system is in a so-called mixed (nonzero-entropy) state initially and $\hat{\rho}$ is diagonal in the energy eigenstate basis, $\hat{H}$ commutes with $\hat{\rho}$ and the Schrödinger term goes to zero even though $\hat{\rho}$ may not be a Maxwellian distribution among the energy eigenlevels. The state evolution of such a mixed-state operator cannot be captured by the Schrödinger term and is instead given by the second term to the right of the equals, the dissipation term, which captures the probability redistribution towards the Maxwellian distribution. The dissipation term is constructed using a set of operators called the 'generators of the motion'. Each generator corresponds to one of the conservation laws to which the system is subjected. For example, an isolated, non-reacting system is subject to two conservation laws, probability normalization and energy conservation, so that the generators of the motion are $\{\hat{I}, \hat{H}\}$, which are the identity operator ($Tr\{\hat{I}, \rho\} = 1$) and the Hamiltonian ($Tr\{\hat{H}, \rho\} = energy$). For the case when $\hat{\rho}$ is diagonal in the energy eigenstate basis, i.e., only the dissipation term is active, the equation of motion takes the form [5]

$$\frac{dp_j}{dt} = \frac{1}{\tau} \frac{\begin{vmatrix} -p_j\ln p_j & p_j & \varepsilon_j p_j \\ \langle s \rangle & 1 & \langle e \rangle \\ \langle es \rangle & \langle e \rangle & \langle e^2 \rangle \end{vmatrix}}{\begin{vmatrix} 1 & \langle e \rangle \\ \langle e \rangle & \langle e^2 \rangle \end{vmatrix}} = \frac{1}{\tau}D_j(\mathbf{p}) \tag{3}$$

where p_j is the diagonal term of $\hat{\rho}$ in the energy eigenstates basis and represents the probability of the system being in the eigenstate associated with the jth energy eigenlevel. Furthermore, $\mathbf{p}$ represents the vector $\{p_j\}$, $\langle \cdot \rangle$ is the expectation value of the property given $\hat{\rho}$, and τ is the relaxation time. This equation is a first order ordinary differential equation of infinite variables $\{p_j\}$. At any instance of time, the expectation value of the property can be calculated via the current $\{p_j\}$ and the energy eigenlevels $\{\varepsilon_j\}$. This equation can be solved using the concept of hypoequilibrium state and/or the density of states method both of which were developed by the authors [9]. A brief introduction to the concept of hypo-equilibrium state is given in Section 2.4.

2.2. System description in phase space

Based on the discipline of statistical mechanics, determining changes in an extensive property such as the energy requires constructing a canonical ensemble composed of microstates with different energy values. Its corresponding intensive properties (e.g., the temperature) can then be calculated via the Maxwellian distribution of the canonical ensemble, and all other thermodynamic properties of the system evaluated using the canonical partition function. To determine changes of both energy and particle number, a grand canonical ensemble must be constructed of microstates with different energy and particle number values. For the study presented here, an isothermal-isobaric ensemble is used to determine changes in volume, and is constructed of microstates with different energy and volume values. A rigorous description of the system using an isothermal-isobaric ensemble [45–49] is presented below using phase space, which is a requirement for the 'density of volume state' calculation for the partition function. Within the SEAQT framework, state space is most generally assumed to be a Hilbert space as in Section 2.1. However, the SEA

principle is applicable to many different types of state spaces [7,51]. Thus, to be consistent with the representation of the isothermal-isobaric ensemble found in the literature for classical/semi-classical systems, the state space representation used here is that of phase space.

Now, consider that a system contains N particles with spin degrees of freedom. The microstate of the system is decided by the position, momentum, and spin of every particle so that the system microstate is a function of $7N$ properties $\{p_{x,i}, q_{x,i}, p_{y,i}, q_{y,i}, p_{z,i}, q_{z,i}, s_i\}$ where $i=1,2,\ldots,N$. By defining a map from the microstate to the system macroscopic property (i.e., a bundle structure [12,51]), each microstate gives a quartet of macroscopic properties, which defines a macrostate. The four properties are particle number (N), energy (e), volume (v) and magnetization (m). The number of microstates with the macroscopic property in the range $e<e'<e+de$, $v<v'<<v+dv$ and $m<m'<<m+dm$ is represented by $\Omega(N,e'<,v'<,m'<)\,dedvdm$, which is the density of states (i.e., the density of microstates per macrostate). In defining the bundle projection from the space of the microstates to that of the macrostate, there should be a unique macroscopic property (N,e,v,m) defined for any microstate to ensure the correct evaluation of density of state in the partition function of the ensemble used (e.g., the isothermal-isobaric ensemble in the present paper). The total particle number N is constant . The total energy (which is only the kinetic energy here) and the total magnetization can be defined by

$$e = \sum_{i=1}^{N} \left(\frac{p_{x,i}^2}{2m_i} + \frac{p_{y,i}^2}{2m_i} + \frac{p_{z,i}^2}{2m_i} \right) \tag{4}$$

$$m = \sum_{i=1}^{N} s_i \tag{5}$$

where the m_i are the particle masses, the $p_{x,i}$, $p_{y,i}$, $p_{z,i}$ are the momentum components of each particle i, and the s_i the particle spins. A unique specification of the exact volume for any given microstate is of great significance to the calculation of the 'density of volume state', which is further needed for the accurate calculation of the partition function of the isobaric-isothermal ensemble (Eq. (49) below). Classically, the volume for a given microstate is given through the concept of a 'shell particle', which can prevent redundancy in the counting of the configurations (i.e., of microstates) for one macrostate and provide the correct 'density of volume state' [53]. However, the 'shell particle' concept fails in quantum mechanics, and, thus, the calculation of the 'density of volume' state is still an open question at the quantum level.

As shown in Fig 1, for a given microstate of a collection of N particles, r_0 is the location of the center of mass. The volume uses a spherical shape and the boundary is decided by the 'shell particle'. All the N particles (the shaded particles) of the system are in the volume $v+dv$ and at least one particle is within the shell volume dv, which describes the outer boundary of the volume v. In this way, the boundary of the systems volume is the solid line, which is a unique choice among all the possible other boundary choices (dashed lines) that could be made that contain the N particles. For further discussion, the reader is refereed to [53–56].

2.3. SEAQT equation of motion

The SEAQT equation of motion in microstate space (phase space) takes the form
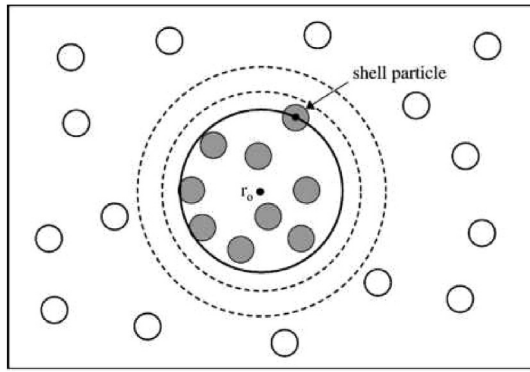
Fig. 1. Definition of volume for a microstate in configuration space using a "shell particle". Reprinted with permission from David S. Corti, Physical Review E, 64(1), 016128, 2001 ©Copyright 2001 by the American Physical Society. 53.

$$\frac{d\rho(p,q,s)}{dt} = \{\rho(p,q,s),H\} + \frac{1}{\tau}D(p,q,s) \qquad (6)$$

where p, q, and s represents all the $7N$ momentum, position, and spin variables in phase space and H is the free particle kinetic energy given by

$$H = e = \sum_{i=1}^{N}\left(\frac{p_{x,i}^2}{2m_i} + \frac{p_{y,i}^2}{2m_i} + \frac{p_{z,i}^2}{2m_i}\right) \qquad (7)$$

The first term on the right in Eq. (6) is the symplectic term (Louisville's equation), while the second is the irreversible relaxation term. The former expressed in terms of the Poisson bracket is written as

$$\{\rho(p,q,s),H\} = \sum_{i=1}^{3N}\left(\frac{\partial\rho}{\partial q_i}\frac{\partial H}{\partial p_i} - \frac{\partial\rho}{\partial p_i}\frac{\partial H}{\partial q_i}\right) = \sum_{i=1}^{3N}\frac{\partial\rho}{\partial q_i}\frac{\partial H}{\partial p_i}$$
$$= \sum_{i=1}^{N}\left(\frac{p_{x,i}}{m_i}\frac{\partial\rho}{\partial q_{x,i}} + \frac{p_{y,i}}{m_i}\frac{\partial\rho}{\partial q_{y,i}} + \frac{p_{z,i}}{m_i}\frac{\partial\rho}{\partial q_{z,i}}\right) \qquad (8)$$

In order to arrive at the equation of motion in macrostate space from which macroscopic properties can directly be obtained, the probability distribution $\tilde{\rho}$ in terms of macroscopic properties (i.e., energy (e), volume (v) and magnetization (m) where the particle number (N) is omitted), as opposed to the probability distribution ρ in phase space, is defined as

$$\tilde{\rho}(e,v,m)dedvdm = \int_{e<e'<e+de,v<v'<v+dv,m<m'<m+dm}\rho(p,q,s)dpdqds \qquad (9)$$

For the specific class of initial conditions studied here in which a generalization of the equal-probability condition for the micro-ensemble holds, the following reasonable approximation for an isotropic nonequilibrium state is valid since there is no favored direction or region of the volume in the system, which can be regarded as the classical one corresponding to the mixed states introduced in the discussion of Eq. (2). Thus,

$$\rho(p,q,s) = \frac{\tilde{\rho}(e,v,m)}{\Omega(e,v,m)}, \text{for all } (p,q,s) \text{ gives the same } (e,v,m) \qquad (10)$$

where

$$\Omega(e,v,m)dedvdm = \int_{e<e'<e+de,v<v'<v+dv,,m<m'<m+dm}dpdqds \qquad (11)$$

is the density of states, i.e., the number of microstates whose macroscopic properties (e',v',m') satisfy the conditions $e<e'<<e+de$, $v<v'<v+dv$ and $m<m'<m+dm$. As a result, the equation of motion of the probability distribution in macroscopic properties takes the form

$$\frac{d\tilde{\rho}(e,v,m)}{dt} = \frac{1}{dedvdm}\int\{\rho(p,q,s),H\}dpdqds$$
$$+ \frac{1}{\tau dedvdm}\int D(p,q,s)dpdqds \qquad (12)$$

for which the integral limits are the same as those for Eqs. (9) and (11), i.e, they include all the microstates providing the same macroscopic properties (e,v,m). Under the equal-probability condition (Eq. (10))

$$\rho(p,q,s) = \rho(-p,q,s) \qquad (13)$$

the relation

$$\int\{\rho(p,q,s),H\}dpdqds = -\int\{\rho(-p,q,s),H\}dpdqds$$
$$= -\int\{\rho(p,q,s),H\}dpdqds = 0 \qquad (14)$$

holds. Clearly, Eq. (14) is only satisfied when the Poisson bracket term vanishes. Furthermore, since the Poisson bracket term in Eq. (12) vanishes at the initial condition, the equal-probability condition holds during the time evolution of the equation of motion, Eq. (6). Thus, Eq. (12) reduces to

$$\frac{d\tilde{\rho}(e,v,m)}{dt} = \frac{1}{\tau dedvdm}\int D(p,q,s)dpdqds \qquad (15)$$

due to the symmetry of this equation. The evolution in macrostate space reveals the irreversible process without the influence of the symplectic term, since it does not affect the system entropy under the conditions specified.

2.4. Nonequilibrium state and evolution description: hypoequilibrium

The thermodynamic features of the nonequilibrium relaxation process generated by the SEAQT framework have a number of useful characteristics, which allow a unique and complete description of each nonequilibrium state via a set of extensive and intensive properties (opposed to via a distribution function only) for the state yielding to Eq. (10). Moreover, the definition of each nonequilibrium intensive property is fundamental relative to the laws of thermodynamics rather than phenomenological. Such a description is based on the key concept of hypoequilibrium state developed by the authors [9,33], which is a direct result of SEA. The physical meaning of hypoequilibrium state is that for a system in a nonequilibrium state, if a subset of its energy eigenlevels are in mutual equilibrium (i.e., the probability distribution for those levels is a Maxwellian distribution), that subset of levels will remain in mutual equilibrium throughout the entire state evolution of the system (i.e., the probability distribution of that subset remains Maxwellian). Thus, a process of relaxation can be described as follows. For any initial state (a distribution of probabilities among

the energy eigenlevels), the eigenlevels can always be regrouped into many subsets such that in every subset the probability distribution is a Maxwellian distribution with a given intensive property (e.g., temperature). However, the different subsets are not necessarily in mutual equilibrium with each other. The number of subsets can be infinite, which is the extreme case when every eigenlevel is by itself a subset. During the system relaxation process, the energy eigenlevels in one subset evolve together to reach mutual equilibrium with the other subsets. The concept of hypoequilibrium state is, thus, well defined for any state of the system and is, fundamental and, therefore, much more general than the local equilibrium assumption. The latter discretizes a global system into many small local systems, each of which is assumed at a phenomenological level to be in a state of equilibrium. In contrast, the hypoequilibrium concept permits each local system to be represented by a nonequilibrium state (even one far-from-equilibrium) for which the probability distribution is a non-Maxwellian distribution.[1] In this section, the mathematical representation of hypoequilibrium is given using a system whose state can be characterized by energy and volume and a Maxwellian distribution with the intensive properties of temperature and pressure. For proofs and a more detailed discussion on the hypoequilibrium state concept, the reader is referred to [9,33].

A probability distribution $\rho(p,q,s)$ among all of the accessible microstates in phase space (represented by $\mathcal{K}$) is used to represent the thermodynamic state of a system (e.g., system A or B in Section 3). If an initial state satisfies the equal-probability condition of Eq. (10), the system state can be represented by a probability distribution $\tilde{\rho}(e,v,m)$ among the accessible set of macrostates (represented by $\mathcal{H}$ and the density of states $\Omega(e,v,m)$), where the number of particles N is a constant for a closed system. By doing so, the microstates (p,q,s) can be studied using the corresponding macrostates (e,v,m) with the result that the number of the dimensions of the state space reduces from $7N$ to 3. Given an initial thermodynamic state $\tilde{\rho}(e,v,m)$, it is proven that the macrostate set $\mathcal{H}$ can be separated into M sets (subsystems),[2] such that the probability distribution in each subsystem yields to a canonical distribution for e and v, i.e.,

$$\forall i = 1, ..., M, \ \tilde{\rho}\left(e^i, v^i, m^i\right)$$
$$= \frac{\tilde{p}^i}{\Lambda^i\left(\beta^i, \theta^i\right)}e^{-\beta^i e^i - \theta^i v^i}, \ \left(e^i, v^i, m^i\right) \in \mathcal{H}_i \tag{16}$$

In this way, each equilibrium state of the system is designated as being in an Mth-order e-v hypoequilibrium state. Based on this definition, any thermodynamic state of the system is a hypoequilibrium state in $\mathcal{H}$ with some order M where M is less than or equal to the number of accessible system macrostates [9,33]. A hypoequilibrium state of order 1 corresponds to a state in stable equilibrium. In Eq. (16), (e^i, v^i, m^i) is one of the macrostates in $\mathcal{H}_i$, β^i and θ^i are intensive properties of $\mathcal{H}_i$, which are the parameters that correspond to the Lagrange multipliers of the energy and volume constraints, $\tilde{p}^i$ is the total probability in subsystem i, and $\Lambda^i(\beta^i, \theta^i)$ is the partition function of the subsystem with parameters β^i and θ^i. Note that since spin is not conserved, there is no corresponding Lagrange multiplier and, thus, no parameter associated with the magnetization m^i. Furthermore, to be complete, $\beta^i=0$ and $\theta^i=0$ if $\#(\mathcal{H}_i) = 1$ (i.e., there is a single macrostate in the ith subsystem) and $\theta^i=0$ if $\#(\mathcal{H}_i) = 2$. Thus, any nonequilibrium state yielding to Eq. (10) can be regarded as a specific M th-order e-v hypoequilibrium state.

Now, the partition function of the ith subspace is written as

$$\Lambda^i\left(\beta^i, \theta^i\right) = \int_{\mathcal{H}_i} \Omega\left(e^i, v^i, m^i\right) e^{-\beta^i e^i - \theta^i v^i} de^i dv^i dm^i$$
$$= \int_{\mathcal{K}_i} e^{-\beta^i e^i - \theta^i v^i} dpdqds \tag{17}$$

where the integral to the right of the first equal sign is over the macrostate set $\mathcal{H}_i$, while that to the right of the second equal sign is over the microstate set $\mathcal{K}_i$, which contains all of the microstates leading to the macrostates in $\mathcal{H}_i$.

For a given Mth-order e-v hypoequilibrium state, the intensive properties of the subsystems can be represented by β^i and θ^i or equivalently using temperature and pressure by

$$T^i = \frac{1}{k_b \beta^i}, \quad P^i = \theta^i T^i \tag{18}$$

A Mth-order e-v hypoequilibrium state can then be represented by a division $\{\mathcal{H}_i(\mathcal{K}_i), i = 1, ..., M\}$ of a system's accessible macrostate (microstate) set and a corresponding triplet set $\{(\tilde{p}^i, \beta^i, \theta^i), i = 1, ..., M\}$. The intensive property set $\{(T^i, P^i), i = 1, ..., M\}$ is a generalization of the definition of intensive property at stable equilibrium (T^{eq}, P^{eq}) to nonequilibrium. Li and von Spakovsky [9,33] prove that if a system begins in an Mth-order hypoequilibrium state, it will remain in an Mth-order hypoequilibrium state throughout the state evolution as long as the same subsystem division is maintained. Thus, the time evolution of the distribution takes the form

$$\forall i = 1, ..., M, \ \left(e^i, v^i, m^i\right) \in \mathcal{H}_i$$

$$\tilde{\rho}\left(e^i, v^i, m^i, t\right) = \frac{\tilde{p}^i(t)}{\Lambda^i\left(\beta^i(t), \theta^i(t)\right)}e^{-\beta^i(t)e^i - \theta^i(t)v^i} \tag{19}$$

Both the intensive property set $\{(T^i(t), P^i(t)), i = 1, ..., M\}$ as well as the triplet set $\{(\tilde{p}^i(t), \beta^i(t), \theta^i(t)), i=1, ..., M\}$ are well defined throughout the entire evolution.

---

[1] The mixing of two rarefied gases flowing in opposite directions can be used as an example. If the gas is sufficiently rare such that particle collisions are unlikely, the assumption that the gas in each location of the mixing region is in equilibrium is a poor one. At each location, two types of particles can always be observed, each with a different temperature based on the direction (+or -) of its velocity. A better approach would be to describe the non-equilibrium (in fact, far-from-equilibrium) state of each local system by a second order hypoequilibrium state, which captures the far-from-equilibrium characteristics of the state based on two temperatures using the fundamental definitions the authors have developed. In this way the state of each local system is characterized by two temperatures that are not geometrically constrained by a particular point within the local system. For the mixing of more than two rarefied gases, a hypoequilibrium state with an order greater than two would be used. Another example would be a system consisting of a chemically reactive gas far from stable chemical equilibrium for which no location in the system can be assumed to be in equilibrium locally. Describing the properties of two or more reactive components individually via the hypoequilibrium concept permits a fundamental characterization of these components via a set of intensive properties (e.g, temperature, chemical potential, etc.). Both examples can be of a homogeneous system for which each local system is in a nonequilibrium state.

[2] This division satisfies $\mathcal{H} = \cup_{i \in \mathcal{I}} \mathcal{H}_i$ and $\mathcal{H}_i \cap \mathcal{H}_j = \varnothing$, where $\mathcal{I}$ is a set of indices, which can be infinite or an uncountable set. M is the number of elements in $\mathcal{I}$. For the extreme case in which every eigenlevel of a continuous spectrum of energy is itself a set, $\mathcal{I}$ is an uncountable set composed of any real number above the ground state and M is infinite. For simplicity, the presentation here is limited to results for a countable set, which means that $i=1, ..., M$, although results can also be developed for an uncountable $\mathcal{I}$.

3. SEAQT for interacting systems

3.1. SEAQT for interacting systems

The equation of motion is designed to study the nonequilibrium relaxation process of an isolated system. However, since interacting systems can be viewed as a composite isolated nonequilibrium system of subsystems whose interactions cause the relaxation process of the composite, the SEAQT equation of motion can be used to determine the evolution of these interacting systems as well.

Now, consider two interacting systems (system A and system B) undergoing a heat as well as a work interaction. The composite system is not in stable equilibrium, and its state is represented by the probability distributions for system A $\{\rho^a(p^a, q^a, s^a)\}$ and for system B $\{\rho^b(p^b, q^b, s^b)\}$ together. There are four conservation laws, which must be satisfied: probability normalization of system A, probability normalization of system B, energy conservation of the composite system, and total volume conservation of the composite system. Based on SEA and the conservation laws, $\{I^a, I^b, H, V\}$ serve as the generators of the motion and the equation of motion for system A takes the form [33,52,57]

$$\frac{d\rho^a(p^a, q^a, s^a)}{dt} = \{\rho^a(p, q, s), H\} + \frac{1}{\tau}D^a(p, q, s) \qquad (20)$$

where

$$H = H^a + H^b$$
$$= \sum_{i=1}^{N_a}\left[\frac{(p_{x,i}^a)^2}{2m_i^a} + \frac{(p_{y,i}^a)^2}{2m_i^a} + \frac{(p_{z,i}^a)^2}{2m_i^a}\right] \qquad (21)$$
$$+ \sum_{i=1}^{N_b}\left[\frac{(p_{x,i}^b)^2}{2m_i^b} + \frac{(p_{y,i}^b)^2}{2m_i^b} + \frac{(p_{z,i}^b)^2}{2m_i^b}\right]$$

and

$$D^a(p, q, s) = \frac{\begin{vmatrix} -\rho^a\ln\rho^a & \rho^a & 0 & e^a\rho^a & v^a\rho^a \\ \langle s\rangle^a & 1 & 0 & \langle e\rangle^a & \langle v\rangle^a \\ \langle s\rangle^b & 0 & 1 & \langle e\rangle^b & \langle v\rangle^b \\ \langle es\rangle & \langle e\rangle^a & \langle e\rangle^b & \langle e^2\rangle & \langle ev\rangle \\ \langle vs\rangle & \langle v\rangle^a & \langle v\rangle^b & \langle ev\rangle & \langle v^2\rangle \end{vmatrix}}{\begin{vmatrix} 1 & 0 & \langle e\rangle^a & \langle v\rangle^a \\ 0 & 1 & \langle e\rangle^b & \langle v\rangle^b \\ \langle e\rangle^a & \langle e\rangle^b & \langle e^2\rangle & \langle ev\rangle \\ \langle v\rangle^a & \langle v\rangle^b & \langle ev\rangle & \langle v^2\rangle \end{vmatrix}} \qquad (22)$$

Here $\rho^{a(b)}$ is the probability distribution in phase space of system A(B), $(p^{a(b)}, q^{a(b)}, s^{a(b)})$ are the variables in system A(B), and $(p, q, s) = (p^a, q^a, s^a, p^b, q^b, s^b)$ are all the variables in the composite system. The macroscopic properties $e^a = e^a(p^a, q^a, s^a)$ and $v^a = v^a(p^a, q^a, s^a)$ are both functions of the microstate (p^a, q^a, s^a) and are calculated according to the bundle structure given by Eq. (4) and the "shell particle" as described in Section 2.2. $\langle \cdot \rangle^{a(b)}$ is the expectation value of a property in system A(B), and $\langle \cdot \rangle = \langle \cdot \rangle^a + \langle \cdot \rangle^b$ is the expectation value of the total property of the composite system. The numerator of the fraction to the right of the equals can be expanded by the elements of the first row and their cofactors such that

$$\det = -\rho^a\ln\rho^a C_1 + \rho^a C_2^a + e^a\rho^a C_3 + v^a\rho^a C_4 \qquad (23)$$

where C_1, C_2^a, C_2^b, C_3, and C_4 are the determinants of the cofactors of

the first line of the numerator's determinant. By defining

$$\frac{C_2^a}{C_1} = -\alpha_a, \quad \frac{C_2^b}{C_1} = -\alpha_b, \quad \frac{C_3}{C_1} = -\beta, \quad \frac{C_4}{C_1} = -\theta \qquad (24)$$

the equation of motion of systems A takes the form

$$\frac{d\rho^a}{dt} = \{\rho^a, H\} + \frac{1}{\tau}(-\rho^a\ln\rho^a - \rho^a\alpha_a - e^a\rho^a\beta - v^a\rho^a\theta) \qquad (25)$$

and similarly for system B

$$\frac{d\rho^b}{dt} = \{\rho^a, H\} + \frac{1}{\tau}\left(-\rho^b\ln\rho^b - \rho^b\alpha_b - e^b\rho^b\beta - v^b\rho^b\theta\right) \qquad (26)$$

where β and θ are the same in the equations of motion for ρ^a and ρ^b, α_a is specific to the equation of motion for ρ^a, and α_b is specific to the equation of motion for ρ^b.

Under the equal-probability condition

$$\rho^a(p^a, q^a, s^a) = \frac{\tilde{\rho}^a(e^a, v^a, m^a)}{\Omega^a(e^a, v^a, m^a)}, \text{ or } \tilde{\rho}^a(e^a, v^a, m^a)$$
$$= \Omega^a(e^a, v^a, m^a)\rho^a(p^a, q^a, s^a) \qquad (27)$$

$$\rho^b\left(p^b, q^b, s^b\right) = \frac{\tilde{\rho}^b\left(e^b, v^b, m^b\right)}{\Omega^b\left(e^b, v^b, m^b\right)}, \text{ or } \tilde{\rho}^b\left(e^b, v^b, m^b\right)$$
$$= \Omega^b\left(e^b, v^b, m^b\right)\rho^b\left(p^b, q^b, s^b\right) \qquad (28)$$

the Poisson bracket vanishes by integrating over all the microstates of the energy e, the volume v, and the magnetization m, and the equation of motion in e-v distribution is written for systems A and B as

$$\frac{d\tilde{\rho}^a}{dt} = \frac{1}{\tau}\left(-\tilde{\rho}^a\ln\frac{\tilde{\rho}^a}{\Omega^a} - \tilde{\rho}^a\alpha_a - e^a\tilde{\rho}^a\beta - v^a\tilde{\rho}^a\theta\right) \qquad (29)$$

$$\frac{d\tilde{\rho}^b}{dt} = \frac{1}{\tau}\left(-\tilde{\rho}^b\ln\frac{\tilde{\rho}^b}{\Omega^b} - \tilde{\rho}^b\alpha_b - e^b\tilde{\rho}^b\beta - v^b\tilde{\rho}^b\theta\right) \qquad (30)$$

In the application to a thermodynamic cycle, system B is assumed to be a temperature reservoir whose properties remain unchanged during its interactions with system A.[3] The following discussion, thus, focuses on the time evolution of system A.

3.2. Equation of motion for two systems in a Mth-order e-v hypoequilibrium state

In order to study how a system in a nonequilibrium state evolves in a thermodynamic cycle, one of two interacting systems, namely, system A, is initialized in a Mth-order e-v hypoequilibrium state. The distribution function among the macrostates of $(e^{a,i}, v^{a,i}, m^{a,i}) \in \mathscr{H}_i^a$ for the ith subsystem ($i = 1, ..., M$) of system A is given by

---

[3] However, this assumption does not mean that the energy flow is reversible, since the heat flow out of system B goes through a temperature gradient that is not infinitesimal. There is no entropy change in system B (i.e., the properties of a reservoir remain unchanged) due to the heat flow, but there is entropy generation in the composite system of systems A and B and the process is irreversible.

$$\tilde{\rho}^{a,i}\left(e^{a,i}, v^{a,i}, m^{a,i}\right) = \frac{\tilde{p}^{a,i}}{\Lambda^{a,i}\left(\beta^{a,i}, \theta^{a,i}\right)} e^{-\beta^{a,i}e^{a,i}-\theta^{a,i}v^{a,i}} \tag{31}$$

where the probability in the ith subsystem of system A ($\tilde{p}^{a,i}$) and the two intensive properties ($\beta^{a,i}$ and $\theta^{a,i}$) define the state of this subsystem and $\Lambda^{a,i}$, which is the partition function for the ith subsystem, is expressed as

$$\Lambda^{a,i}\left(\beta^{a,i}, \theta^{a,i}\right) = \int\limits_{\mathcal{H}^{a,i}} \Omega\left(e^{a,i}, v^{a,i}, m^{a,i}\right) e^{-\beta^{a,i}e^{a,i}-\theta^{a,i}v^{a,i}} de^{a,i}dv^{a,i}dm^{a,i}$$
$$= \int\limits_{\mathcal{K}^{a,i}} e^{-\beta^{a,i}e^{a,i}-\theta^{a,i}v^{a,i}} dpdqds \tag{32}$$

Defining

$$\alpha^{a,i} = \ln \Lambda^{a,i}\left(\beta^{a,i}, \theta^{a,i}\right) - \ln \tilde{p}^{a,i} \tag{33}$$

the ith subsystem state can be represented by

$$\tilde{\rho}^{a,i}\left(e^{a,i}, v^{a,i}, m^{a,i}\right) = e^{-\alpha^{a,i}} e^{-e^{a,i}\beta^{a,i}} e^{-v^{a,i}\theta^{a,i}} \tag{34}$$

The equation of motion (Eq. (29)) takes the form

$$\frac{d\tilde{\rho}^{a,i}}{dt} = \frac{1}{\tau}\left(-\tilde{\rho}^{a,i}\ln\frac{\tilde{\rho}^{a,i}}{\Omega^{a,i}} - \tilde{\rho}^{a,i}\alpha_a - e^{a,i}\tilde{\rho}^{a,i}\beta - v^{a,i}\tilde{\rho}^{a,i}\theta\right) \tag{35}$$

where the superscript 'i' indicates the ith subsystem. As is proven in Refs. [9,33], if the initial state is a hypoequilibrium state, the system remains in a hypoequilibrium state provided the same subsystem division is maintained. As a consequence, the time evolution of the distribution of the ith subsystem of A takes the form

$$\tilde{\rho}^{a,i}(t) = e^{-\alpha^{a,i}(t)} e^{-e^{a,i}\beta^{a,i}(t)} e^{-v^{a,i}\theta^{a,i}(t)} \tag{36}$$

where $\alpha^{a,i}(t), \beta^{a,i}(t), \theta^{a,i}(t)$ are the solution of

$$\frac{d\alpha^{a,i}}{dt} = -\frac{1}{\tau}\left(\alpha^{a,i} - \alpha_a\right) \tag{37}$$

$$\frac{d\beta^{a,i}}{dt} = -\frac{1}{\tau}\left(\beta^{a,i} - \beta\right) \tag{38}$$

$$\frac{d\theta^{a,i}}{dt} = -\frac{1}{\tau}\left(\theta^{a,i} - \theta\right) \tag{39}$$

By solving these three equations of motions for each ith subsystem, the time evolution of system A is obtained ($3M$ equations in total). The parameters β and θ, which are determined by Eq. (24), are expressed using the intensive and extensive properties of both system A and system B, namely $\langle e \rangle^{a(b)}, \langle v \rangle^{a(b)}, \alpha^{a(b),i}, \beta^{a(b),i}$ and $\theta^{a(b),i}$.

3.3. Interacting with a reservoir

Assuming system B, which is in a stable equilibrium state with parameters β_r and θ_r, to have a volume and energy much larger than that of system A, Ref. [33] proves that the parameters in Eqs. (38) and (39) take the form

$$\beta = \beta_r, \quad \theta = \theta_r \tag{40}$$

so that the equations of motion of the ith subsystem of system A are rewritten as

$$\frac{d\alpha^{a,i}}{dt} = -\frac{1}{\tau}\left(\alpha^{a,i} - \alpha_a\right) \tag{41}$$

$$\frac{d\beta^{a,i}}{dt} = -\frac{1}{\tau}\left(\beta^{a,i} - \beta_r\right) \tag{42}$$

$$\frac{d\theta^{a,i}}{dt} = -\frac{1}{\tau}\left(\theta^{a,i} - \theta_r\right) \tag{43}$$

where α_a is determined from an expansion of the determinants that define the numerator and denominator of Eq. (24). The result using Eq. (40) reduces to the following:

$$\alpha_a = \sum_i \alpha^{a,i}\tilde{p}^i \sum_i \langle e \rangle^{a,i}\beta^{a,i} + \sum_i \langle v \rangle^{a,i}\theta^{a,i} - \beta_r\langle e \rangle^a - \theta_r\langle v \rangle^a \tag{44}$$

where $\langle \cdot \rangle^{a,i}$ is the contribution of the ith subspace to the extensive properties of system A. Thus, only the intensive properties of the reservoir (system B) appear in the equation of motion of system A in the form of the reservoir parameters β_r and θ_r, and this equation is independent of the type of component (represented by the extensive properties ($\langle e \rangle^b, \langle v \rangle^b$)) present in the reservoir.

4. Cycle of the system undergoing a nonquasi-equilibrium process

This section provides an example of the use of SEAQT in the modeling of a thermodynamic cycle going through nonquasi-equilibrium process. SEAQT model development requires a definition of the system [39], which contains the particles and the Hamiltonian, which defines the energy eigenlevels or accessible microstates in phase space. The density of states (Ω from Eq. (11)) and partition function (Λ from Eq. (17)) can then be determined. All the extensive properties (e.g., $\langle e \rangle$ and $\langle v \rangle$) at a given thermodynamics state (i.e., probability distribution) can be found. The relaxation time in the equation of motion is chosen based on the interactions or phenomena studied. It can be calculated from mechanics (e.g., kinetic theory) or directly from the experimental data of phenomenological coefficients (e.g., the diffusion coefficient or reaction rate constant) [10,32], which allows a comparison with experiment [36,58,59]. However, the results presented here, which show the general thermodynamic features of system nonequilibrium behavior, do not change when the relaxation time changes, i.e., the kinetic behavior of the system is independent of its dynamic behavior. The latter simply places the kinetic behavior in the correct timescale.

To model a specific process, an initial condition is chosen, i.e., a hypoequilibrium state and the initial intensive properties for each subsystem.[4] The equation of motion provides the time evolution from a nonequilibrium state to a stable equilibrium state for an isolated system or the time evolution from a transient to a steady cycle for a cyclic process as shown below. The intermediate states in the evolution can be calculated without the relaxation time, while the relaxation time can map the intermediate states onto the correct time scale. For the study below, the time-related parameter is

---

[4] For example, for a counterflow of rarefied gas, two subsystem with different temperatures and pressures ($\beta^{a,i}$ and $\theta^{a,i}$ in Eq. (31)) can be used, and the total probabilities ($\tilde{p}^{a,i}$ in Eq. (31)) in each subsystem can be determined from the relative value of the flow rate.

the ratio of the characteristic time of the reservoir (τ_r, i.e., the period of the piston) to the characteristic time of system relaxation (τ, determined by a phenomenological transport coefficient, e.g., the diffusion coefficient [10]). The result is general for systems of different constituents but the same τ_r/τ.

4.1. System description and initial state

The cyclic process is studied using a nonequilibrium system (system A) interacting with a series of reservoirs (systems B) as shown in Fig. 2. System A consists of approximately 1 mole Helium-3 in a piston-cylinder with variable energy and volume interacting with a different temperature reservoir at each instant of time t. The reservoir at a given t has the intensive properties $(T(t),P(t))$ where T is the temperature and P the pressure. At any given instant of time, the interaction between system A and system B keeps the total energy and volume of the composite system of A and B conserved. When the temperature is not too low, Helium-3 performs as a Maxwellian particle.

In order to simplify the discussion, a special nonequilibrium initial condition, whose analytical solution is available, is used. For other initial nonequilibrium states in a more general application, the evolution can be solved with Eq. (3) or (15) using the density of states method [9]. The number of particles in system A is assumed to be odd, and the initial state of system A is chosen to be a second-order e-v hypoequilibrium state. The corresponding two subspaces are chosen to be the set of all macrostates with the magnetization $m>0$ so that $\{(e^\uparrow, v^\uparrow, \uparrow)\}$ and the set of all macrostates with $m<0$ so that $\{(e^\downarrow, v^\downarrow, \downarrow)\}$. For this division of the system, the partition functions for the two subspaces are the same as are the extensive property functions, which facilitates comparison of the two subsystems, especially of the extensive properties like energy and volume. Higher order e-v hypoequilibrium states can also be studied and for more details, the reader is referred to [33]. The initial state can be represented by the macrostate probability distributions of each of the subspaces, i.e., by $\{\tilde{p}^\uparrow\}$ and $\{\tilde{p}^\downarrow\}$, where

$$\tilde{\rho}^\uparrow = \frac{\tilde{p}^\uparrow}{\Lambda^\uparrow\left(\beta^\uparrow, \theta^\uparrow\right)} e^{-e^\uparrow \beta^\uparrow} e^{-v^\uparrow \theta^\uparrow} \tag{45}$$

$$\tilde{\rho}^\downarrow = \frac{\tilde{p}^\downarrow}{\Lambda^\downarrow\left(\beta^\downarrow, \theta^\downarrow\right)} e^{-e^\downarrow \beta^\downarrow} e^{-v^\downarrow \theta^\downarrow} \tag{46}$$

Here $(\tilde{p}^\uparrow, \beta^\uparrow, \theta^\uparrow)$ is the parameter triplet for the $m>0$ subspace and $(\tilde{p}^\downarrow, \beta^\downarrow, \theta^\downarrow)$ for the $m<0$ subspace defined in Section 3.2. Both the partition function for the $m>0$ subspace and that for the $m<0$ subspace share the same functional form Λ_0 so that
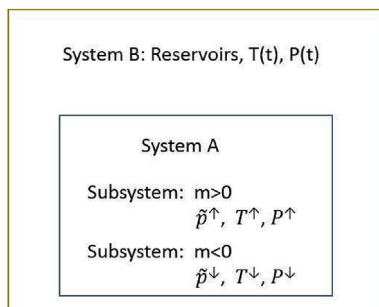
Fig. 2. System model.

$$\Lambda^{\uparrow(\downarrow)}\left(\beta^{\uparrow(\downarrow)}, \theta^{\uparrow(\downarrow)}\right) = \Lambda_0\left(\beta^{\uparrow(\downarrow)}, \theta^{\uparrow(\downarrow)}\right) \tag{47}$$

while the partition function for the total system is given by

$$\Lambda^{total}(\beta, \theta) = \Lambda^\uparrow(\beta, \theta) + \Lambda^\downarrow(\beta, \theta) = 2\Lambda_0(\beta, \theta) \tag{48}$$

where

$$\begin{aligned}\Lambda^{total}(\beta, \theta) &= \int_{\mathscr{H}} \Omega(e, v, m) e^{-\beta e - \theta v} de\, dv\, dm \\ &= \int_{\mathscr{K}} e^{-\beta e - \theta v} dp\, dq\, ds\end{aligned} \tag{49}$$

Note that the evaluation of the partition function is based on the concept of the density of volume state $\Omega(e,v,m)$[60] for an isothermal-isobaric ensemble partition function [53—56]. Thus, using the formulation provided in [54]

$$\begin{aligned}\Lambda^{total}(\beta, \theta) &= \int_v \left(\frac{\partial \ln Q}{\partial v}\right)_{T,N} Q e^{-\theta v} dv \\ &= \int_v \left(\frac{\partial Q}{\partial v}\right)_{T,N} e^{-\theta v} dv = \int_v e^{-\theta v} dQ\end{aligned} \tag{50}$$

where Q is the canonical ensemble partition function for a system containing N particles in a volume v at temperature T. For Maxwellian particles with a spin degeneracy of 2, Q takes the following form when the non-degenerate form given in Ref. [53] is modified:

$$Q = \frac{2^N}{N!}\left(\frac{\sqrt{2\pi m}}{h}\right)^{3N} v^N \beta^{-\frac{3}{2}N} \tag{51}$$

Λ^{total} then takes the form

$$\begin{aligned}\Lambda^{total}(\beta, \theta) &= \frac{2^N}{(N-1)!}\left(\frac{\sqrt{2\pi m_{He-3}}}{h}\right)^{3N} \beta^{-\frac{3}{2}N} \int_0^\infty v^{N-1} e^{-\theta v} dv \\ &= 2^N \left(\frac{\sqrt{2\pi m_{He-3}}}{h}\right)^{3N} \beta^{-\frac{3}{2}N} \theta^{-N}\end{aligned} \tag{52}$$

where m_{He-3} is the mass of a Helium-3 particle. Furthermore, the extensive properties of one subsystem of system A and those of the entire system A are written as

$$\langle e \rangle^{\uparrow(\downarrow)} = p^{\uparrow(\downarrow)}\left(-\frac{1}{\Lambda^{\uparrow(\downarrow)}} \frac{\partial \Lambda^{\uparrow(\downarrow)}}{\partial \beta}\right) = \frac{3N\tilde{p}^{\uparrow(\downarrow)}}{2\beta^{\uparrow(\downarrow)}} \tag{53}$$

$$\langle V \rangle^{\uparrow(\downarrow)} = \tilde{p}^{\uparrow(\downarrow)}\left(-\frac{1}{\Lambda^{\uparrow(\downarrow)}} \frac{\partial \Lambda^{\uparrow(\downarrow)}}{\partial \theta}\right) = \frac{N\tilde{p}^{\uparrow(\downarrow)}}{\theta^{\uparrow(\downarrow)}} \tag{54}$$

$$\langle e \rangle = \langle e \rangle^\uparrow + \langle e \rangle^\downarrow \tag{55}$$

$$\langle v \rangle = \langle v \rangle^\uparrow + \langle v \rangle^\downarrow \tag{56}$$

Since the time evolution of a reservoir due to its interaction with system A is negligible, the study focuses on the evolution of system A provided by the equation of motion for system A (Eqs. (41) to (43)).

4.2. Relaxation time τ

Depending on which type of interaction is being modeled, the relaxation time τ can be estimated using fundamental transport information such as a diffusion coefficient, a chemical reaction rate constant [10,61], or a viscosity. The self-diffusion coefficient is used here as an example. If it is assumed that diffusion dominates the relaxation of the system, the relation between the system relaxation time and its self-diffusion coefficient D_{self} as derived in Ref. [10] is given by

$$\tau = \frac{(\delta x)^2}{2D_{self}} \tag{57}$$

where δx is the distance between the center of the interacting systems (approximated by the dimension of system A here) and $D_{self}=D_{self}(P,T)$ is a function of the pressure P and the temperature T. The dependence of the diffusion coefficient on temperature for gases is based on the Chapman-Enskog theory. For the binary diffusion of A and B, the diffusion coefficient is

$$D_{AB} = \frac{0.0018583 T^{3/2}\sqrt{1/M_A + 1/M_B}}{P\sigma_{AB}^2 \Omega} \tag{58}$$

where M_A and M_B are the standard atomic weight, P [atm] is the pressure, T [K] is the temperature, σ_{AB}[Å] is the average collision diameter, and Ω is a temperature-dependent collision integral. In the case of the self-diffusion of Helium-3, the parameters of A and B are both chosen to be that of the Helium-3 molecule, while σ_{AB}[Å] and Ω are both tabulated [62]. For simplicity, the average self-diffusion coefficient for Helium-3 at the end-cycle is used to get the order of magnitude for a constant τ. For Helium-3 at 4atm and 1500 K, $\tau\sim70$ s. The SEAQT model can accommodate a state-dependent τ (e.g., via Eqs. (57) and (58) and instantaneous pressures and temperatures) to provide a more complete time evolution for a specific system. However, the focus here is on the general thermodynamic features and, thus, using the relative order of magnitude of the relaxation time and cycle period is sufficient. Furthermore, the ratio of the cycle period τ_r (defined later) to the relaxation time is a non dimensional number describing the relative speed of the reservoir's operation to the characteristic time scale of a specific interaction. It takes the form

$$\frac{\tau}{\tau_r} = \frac{(\delta x)^2}{2D_{self}\tau_r} \tag{59}$$

4.3. Reservoir

The reservoir series $(T(t),P(t))$ is defined to be a periodic function of time with period τ_r, where τ_r is the periodic of system B changing, i.e., the characteristic time of system B. Thus,

$$T(t) = T(t-\tau_r) \quad \text{if } t \ge \tau_r \tag{60}$$

$$P(t) = P(t-\tau_r) \quad \text{if } t \ge \tau_r \tag{61}$$

In one period τ_r, $(T(t),P(t))$ are expressed as

$$P(t)=\begin{cases} P_1 & \text{if } 0 \le t < 0.25\tau_r \\ P_1+(P_2-P_1)\dfrac{t-0.25\tau_r}{0.25\tau_r} & \text{if } 0.25\tau_r \le t < 0.5\tau_r \\ P_2 & \text{if } 0.5\tau_r \le t < 0.75\tau_r \\ P_2+(P_1-P_2)\dfrac{t-0.75\tau_r}{0.25\tau_r} & \text{if } 0.75\tau_r \le t < \tau_r \end{cases} \tag{62}$$

$$T(t)=\begin{cases} T_1+(T_2-T_1)\dfrac{t}{0.25\tau_r} & \text{if } 0 \le t < 0.25 \\ P(t)T_2/P_1 & \text{if } 0.25\tau_r \le t < 0.5\tau_r \\ T_3+(T_4-T_3)\dfrac{t-0.5\tau_r}{0.25\tau_r} & \text{if } 0.5\tau_r \le t < 0.75\tau_r \\ P(t)T_4/P_2 & \text{if } 0.75\tau_r \le t < \tau_r \end{cases} \tag{63}$$

The trajectory of $(T(t),P(t))$ on a P-T diagram is shown in Fig. 3. If the intensive properties of system A were to proceed through a quasi-equilibrium process, its trajectory on a P-V diagram would be that shown in Fig. 4.
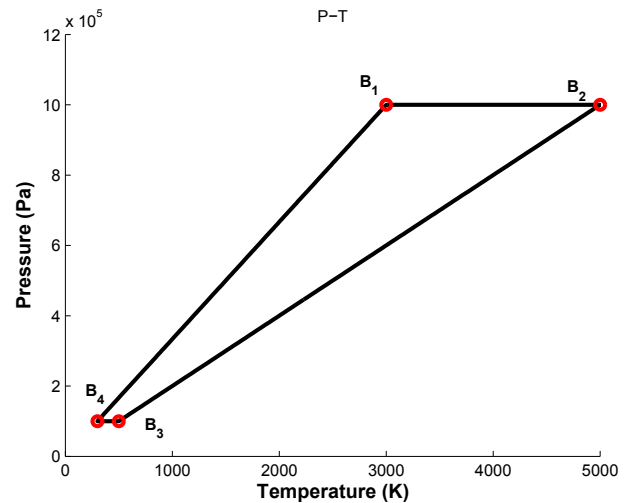
Fig. 3. Reservoir locations on a P-T diagram. B_1 to B_4 represent the stable equilibrium states of the system at different (T,P). B_1:(3000 K,10^6 Pa). B_2:(5000 K,10^6 Pa). B_3:(500 K,10^5 Pa). B_4:(300 K,10^6 Pa).
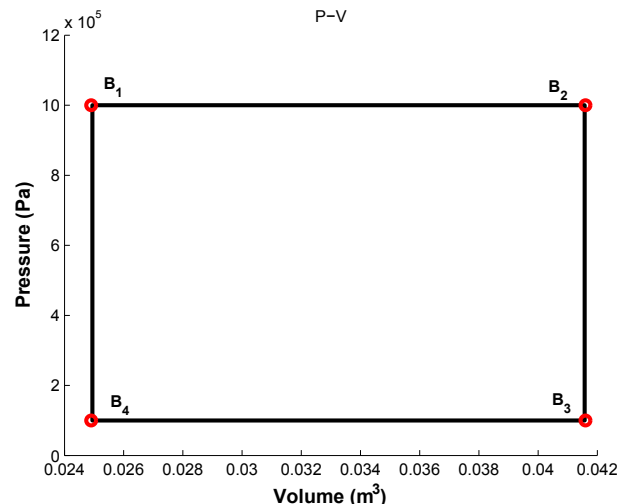
Fig. 4. Reservoir locations on a P-V diagram.

5. Results

5.1. Transient process

The SEAQT model is used to study how a system proceeds through a cycle formed by two constant-pressure and two constant-volume processes. The traditional way is to assume that the system is at stable equilibrium at every instant of time so that it follows the path of a quasi-equilibrium process. Such a path is represented by the black lines in Figs. 3—7. As shown later, this is the limiting path that system B (i.e., the reservoirs) follows as it changes very, very slowly. In the general case, the nonequilibrium interactions of system A with the reservoir result in a different path. Using the SEAQT nonequilibrium model, three cases with different characteristic times for system B ($\tau_r/\tau = 50, 5, 0.5$) are simulated. The model predictions clearly illustrate that as system B changes more quickly, the behavior of system A departs ever further from the quasi-equilibrium process.

Cycle diagrams for systems A and B are given in Figs. 5—7. Since the system is in a nonequilibrium state initially and throughout its state evolution, temperature and pressure are generally not defined. However, using a second-order e-v hypoequilibrium state description as discussed in Section 2, the temperature and pressure for each subsystem can be found so that a comparison of the pressure and temperature evolutions for the $m>0$ subsystem, $m<0$ subsystem, and reservoir can be made. The contribution to the volume of system A can be calculated for each subsystem. Normalizing by the probabilities of each subsystem, the $m>0$ subsystem, $m<0$ subsystem, and system B (reservoirs) evolutions can also be compared on a P-V diagram.

Two general features can be observed from the P-T and P-V diagrams of Figs. 5—7. The first is that the red and blue lines, which represent the $m>0$ and $m<0$ subsystems, respectively, start from two different locations on the diagrams and converge at the end. This represents the process of system A evolving from some nonequilibrium state to stable equilibrium or, equivalently, it is the process that the two subsystems of system A undergo to come to mutual stable equilibrium with each other.

The second general feature is that after the two subsystems arrive at mutual stable equilibrium, the two converged lines (i.e., the red and the blue) can be regarded as the nonquasi-equilibrium path that system A would follow if each of its states were in stable equilibrium at any instant of time. The terminology "nonquasi-equilibrium" refers to the fact that system A and system B are not
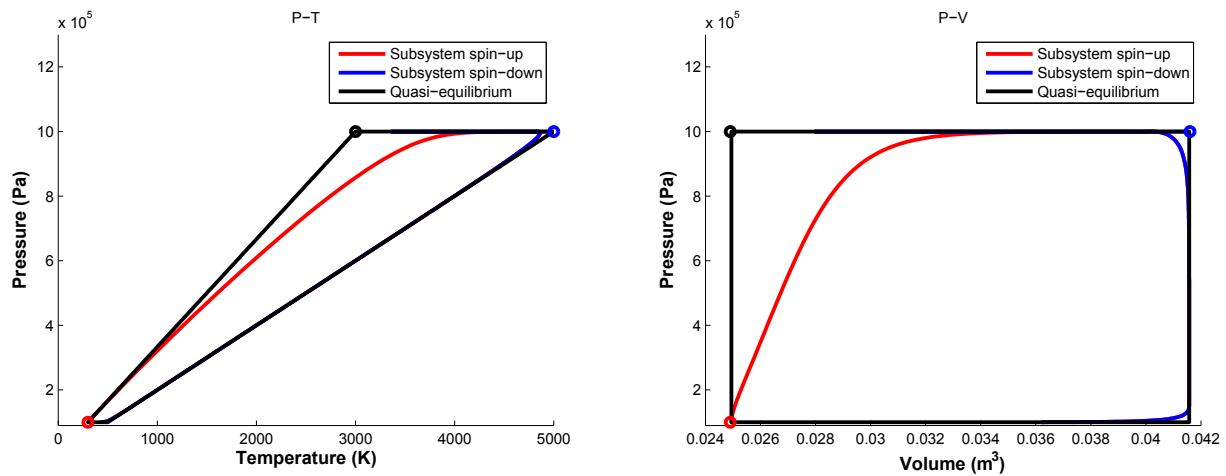
Fig. 5. P-T and P-V cycle diagrams for $\tau_r/\tau = 50$ with the red/blue/black dots representing the initial states for the $m>0$ subsystem, the $m<0$ subsystem, and system B, respectively. System B evolves clockwise. (For interpretation of the references to colour in this figure legend, the reader is referred to the web version of this article.)
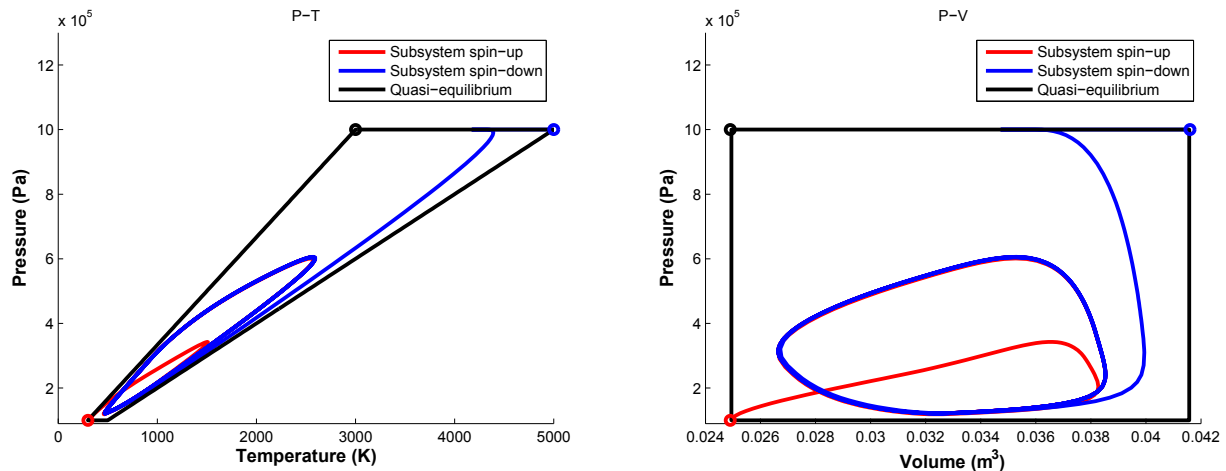
Fig. 6. P-T and P-V cycle diagrams for $\tau_r/\tau = 5$ with the red/blue/black dots representing the initial states for the $m>0$ subsystem, the $m<0$ subsystem, and system B, respectively. System B evolves clockwise. (For interpretation of the references to colour in this figure legend, the reader is referred to the web version of this article.)
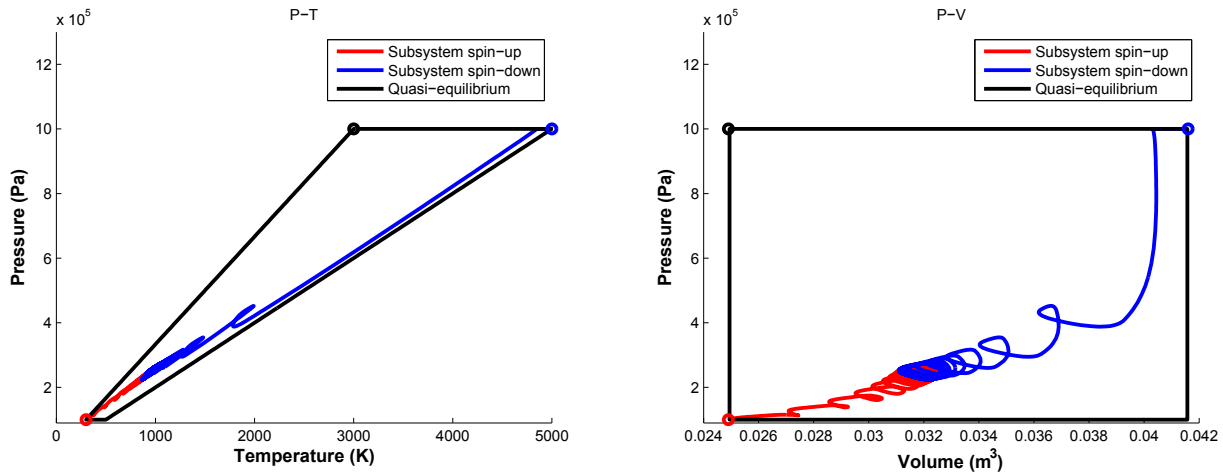
Fig. 7. *P-T* and *P-V* cycle diagrams for $\tau_r/\tau = 0.5$ with the red/blue/black dots representing the initial states for the $m>0$ subsystem, the $m<0$ subsystem, and system B, respectively. System B evolves clockwise. (For interpretation of the references to colour in this figure legend, the reader is referred to the web version of this article.)

always in mutual equilibrium, and that the composite system is not in stable equilibrium. This path called the end-cycle (i.e., the steady as opposed to transient cycle) is generally different from the cycle path that system B takes. This end-cycle or steady cycle can have a great deal of overlap with the cycle path of system B such as occurs in Fig. 5 or it can have almost no overlap such as occurs in Figs. 6 and 7. Note that the composite system of A and B is in a nonequilibrium state, even one far from equilibrium, so that the interactions between system A and B are not restricted to those in the near-equilibrium region. The difference in the cycles of these two systems results from the fact that they are not in mutual equilibrium and from the fact that the nonequilibrium intensive properties of system A are very different from the equilibrium properties of system B. Furthermore, the ratio of τ_r to τ indicates how strong the interactions between system A and system B are compared to with how fast system B changes its state. If τ_r/τ is sufficiently large, the interactions between A and B are strong enough to make systems A and B come to mutual stable equilibrium before there is a change in reservoir as seen in Fig. 5. In contrast, when this ratio is sufficiently small as in Figs. 6 and 7, systems A and B are not able to reach mutual stable equilibrium before there is a change in reservoir.

A comparison across Figs. 5–7 shows how the ratio τ_r/τ influences the end-cycle. When this ratio is small, so is the end-cycle resulting in less work produced by the cycle (or less heat absorbed by the cycle when it operates in reverse) as indicated by the cycle area on the *P-V* diagram. In other words, as the characteristic time of the series of reservoirs represented by system B becomes smaller, the work done by system A becomes smaller and the loss in work is the difference between the area of the end-cycle and that of the cycle of system B. To achieve a better cyclic device design, the characteristic time of the series of reservoirs should be considerably larger than the characteristic time for the interactions as is the case in Fig. 5. Furthermore, for the limiting case when τ_r/τ becomes very small as in Fig. 7, system A interacts with a fast-changing system B (i.e., series of reservoirs), which is equivalent to the case when system A interacts with a single reservoir, whose intensive properties are the average of the system B cycle. Thus, changes of the single reservoir only appear as fluctuations.

Finally, in Fig. 8, the pressure, temperature, and entropy evolutions for two cases, $\tau_r/\tau=50$ and $\tau_r/\tau=5$, are compared. As indicated earlier, the time for the red and blue lines to converge is the time for the two subsystems of system A to reach mutual stable equilibrium. This is also the approximate start time for the end-cycle (see Figs. 6

and 7). As seen in Fig. 8, for a ratio of $\tau_r/\tau=50$, system A takes longer to arrive at the end-cycle (steady cycle) for the reason that the $m<0$ subsystem is driven by the series of reservoirs to approach state B_2 (5000 K, 10^6 Pa), while for the $\tau_r/\tau=5$ case, this same subsystem is driven to approach state B_3 (500 K, 10^5 Pa) because the constant-pressure process has already finished by the time that this subsystem's temperature has reached a peak at a dimensionless time of approximately 2. It is also observed that, for the steady cycle, the changing range of temperature and pressure for the $\tau_r/\tau=5$ case is inside of that for the $\tau_r/\tau=50$ case. This is consistent with the result from Figs. 5–7 in which the end-cycle for the $\tau_r/\tau=5$ case is inside of that for the $\tau_r/\tau=50$ case.

5.2. Steady cycle

For a steady cycle at a given τ_r/τ, one can determine the maximum and minimum of the volume and entropy, and then separate the cycle on *P-V* and *T-S* diagrams into upper and lower parts, i.e., into half-cycles, as is done in Fig. 9. By defining the work and heat interactions of a half cycle, which correspond to either inputs (or outputs) depending on the given direction of the cyclic evolution (clockwise for a heat engine and counter-clockwise for a heat pump), i.e.,

$$W_{upper} = \int_{upper-half-cycle} PdV \tag{64}$$

$$W_{lower} = \int_{lower-half-cycle} PdV \tag{65}$$

$$W_{net} = W_{upper} - W_{lower} \tag{66}$$

$$Q_{upper} = \int_{upper-half-cycle} TdS \tag{67}$$

$$Q_{lower} = \int_{lower-half-cycle} TdS \tag{68}$$

$$Q_{net} = Q_{upper} - Q_{lower} \tag{69}$$

the efficiency of the cycle can be evaluated by the ratio of work to heat for a heat engine and heat to work for a heat pump. For the latter, the efficiency for a cycle consisting of two constant-pressure
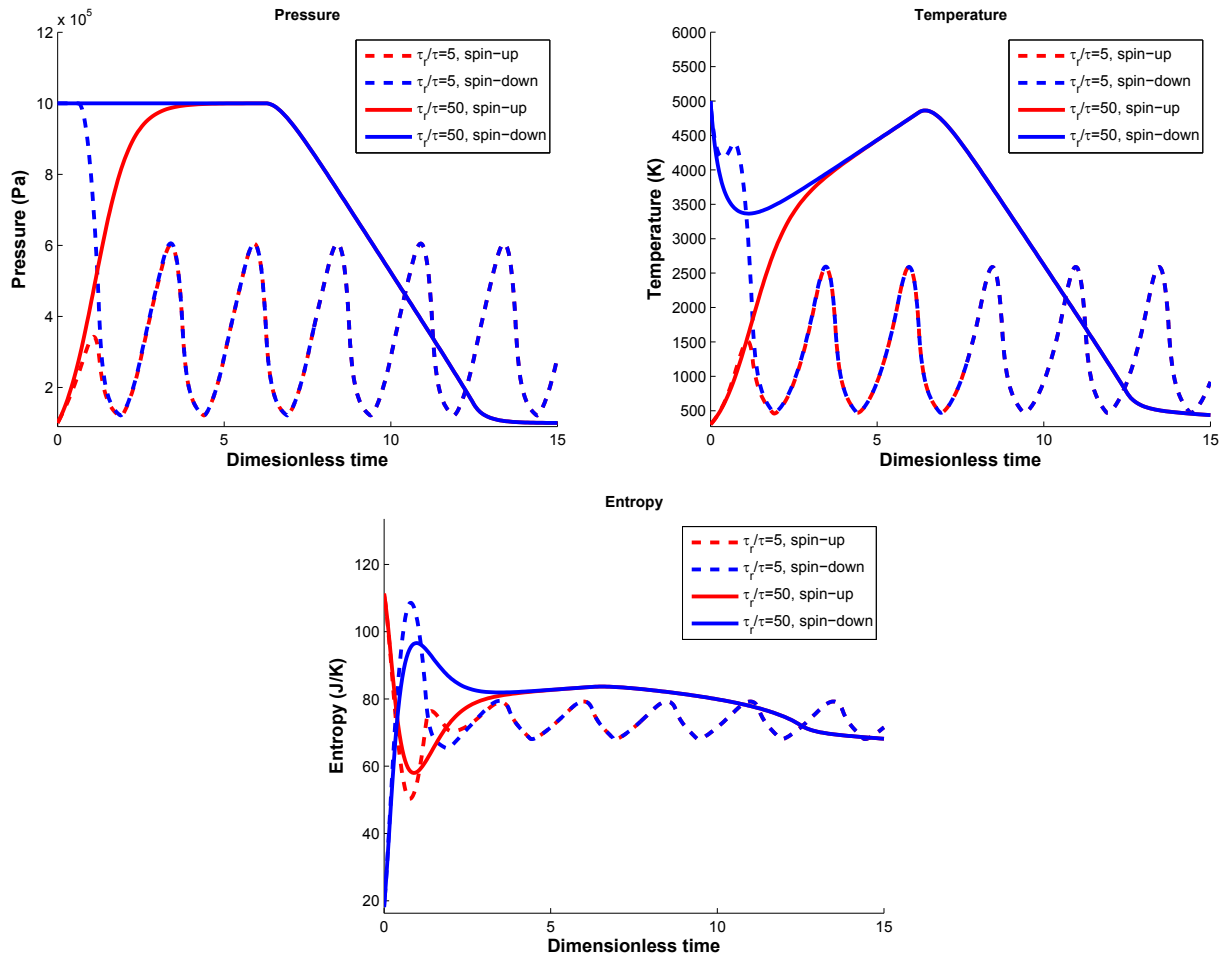
Fig. 8. Pressure, temperature, and entropy evolution for the $\tau_r/\tau=50$ and $\tau_r/\tau=5$ cases.
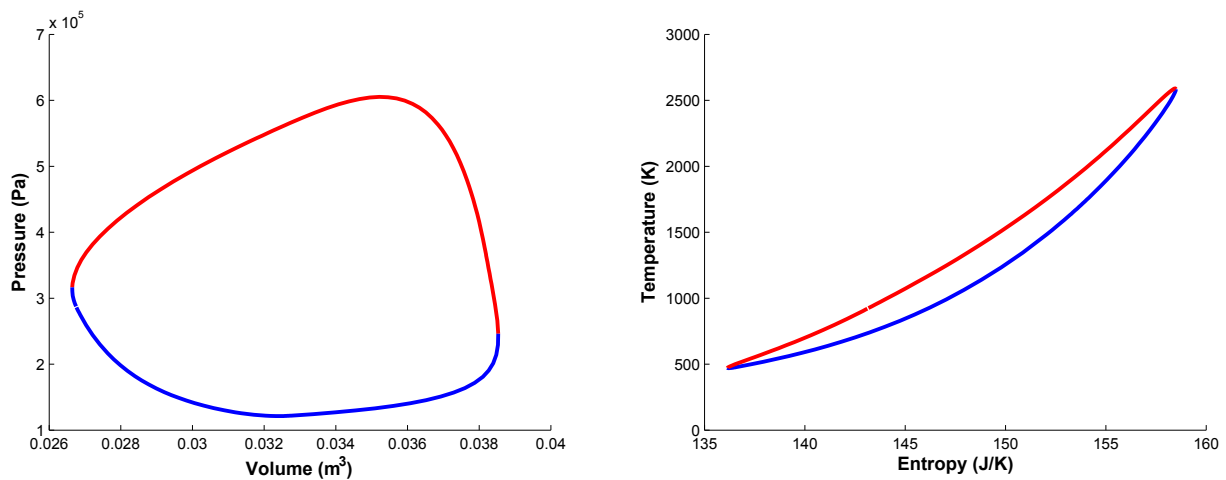
Fig. 9. The upper half of the cycle (red line) and lower half of the cycle (blue line) on *P-V* and *T-S* diagrams for the end-cycle for $\tau_r/\tau=5$. (For interpretation of the references to colour in this figure legend, the reader is referred to the web version of this article.)

and two constant-volume processes is given by the ratio of the net heat (Eq. (66)) to the work of the upper cycle (Eq. (61)), i.e., the work input. This efficiency reaches a maximum when the composite system goes through a quasi-equilibrium cycle, i.e., when τ_r/τ becomes large, which is an ideal cycle working between two pressure reservoirs (see the rectangle in Fig. 6a). For a given net

heat, the work input reaches a minimum when the cycle acts as a heat pump. Thus, the efficiency defined by

$$\varepsilon_{heat\ pump} = \frac{Q_{net}}{W_{input}} = \frac{W_{net}}{W_{input}} \tag{70}$$
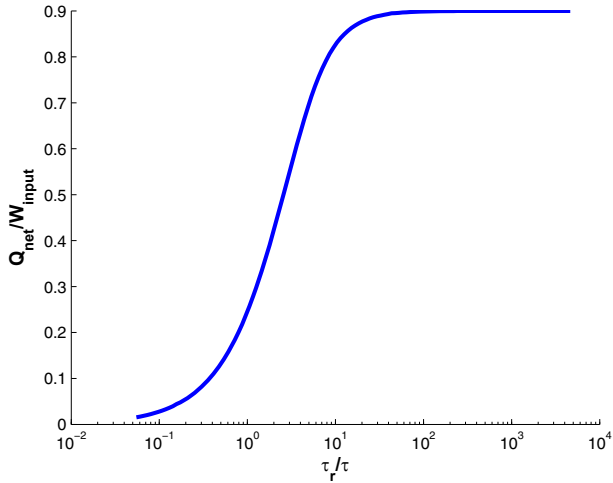
Fig. 10. Nonequilibrium effects on efficiency.

can be used as an indicator of how strong the nonequilibrium effects in the system are. The efficiency for the quasi-equilibrium cycle is given by

$$\varepsilon_{heat\ pump}^{quasi} = \frac{Q_{net}^{quasi}}{W_{input}^{quasi}} = \frac{W_{net}^{quasi}}{W_{input}^{quasi}} = 1 - \frac{P_{min}}{P_{max}} \tag{71}$$

where

$$W_{input}^{quasi} = P_{max}\Delta V \tag{72}$$

$$Q_{net}^{quasi} = W_{net}^{quasi} = (P_{max} - P_{min})\Delta V \tag{73}$$

and $\Delta V = V_{max} - V_{min}$. Note that the efficiency for the heat engine given by the ratio of the net work to the heat input also has a maximum but not one that coincides with that of the quasi-equilibrium cycle involving two constant-pressure and two constant-volume processes. For the maximum to coincide with that of the quasi-equilibrium cycle requires a cycle consisting of two constant-temperature and two constant-entropy processes, i.e., the

so-called Carnot cycle, for which the maximum efficiency is expressed as

$$\varepsilon_{heat\ engine}^{quasi} = \frac{W_{net}^{quasi}}{Q_{input}^{quasi}} = \frac{Q_{net}^{quasi}}{Q_{input}^{quasi}} = 1 - \frac{T_{min}}{T_{max}} \tag{74}$$

Fig. 10 shows the variation in heat pump efficiency $\varepsilon_{heatpump}$ with τ_r/τ. This efficiency changes significantly in the τ_r/τ range of 10^{-1} to 10^1, which indicates that the reservoir influences the efficiency the most when the period of the reservoir (or cycle) τ_r and the relaxation time τ of the rate of the non-equilibrium relaxation between the subsystems of the cycle (system A) and the reservoir (system B) are compatible. Furthermore, the net power or rate of net work of the cycle defined as

$$\dot{W}_{net} = \frac{W_{net}}{\tau_r} \tag{75}$$

can be optimized. As seen in Fig. 10, the efficiency of the heat pump cycle increases monotonically as the period of the reservoir τ_r increases, while the net power as given by Eq. (72) decreases.

Fig. 11 shows that the maximum net power is reached at about 10^1 at which point the heat pump efficiency has not yet reached its maximum. Further increases of τ_r/τ increase the efficiency to its maximum; but decreases in the non-equilibrium effects occur at a continually decreasing rate, which contrasts with the time consumed per cycle, which increases at a steady rate. The result is that an optimal balance between the nonequilibrium effects and the speed of the cycle τ_r yields a maximum net power point as seen in Fig. 11 (red dashed line). This peak, of course, is influenced by the maximum and minimum reservoir pressures; and for a system with a given relaxation time τ working between two pressure reservoirs, the cycle period can, if desired, be optimized to produce the maximum net rate of heat transfer for the cycle. Conversely, this same period can be optimized to maximize cycle efficiency instead with a consequent reduction in nonequilibrium effects.

5.3. Error analysis

The solver for the ordinary differential equations used here is ode45 in Matlab with an absolute error of less than 10^{-100} and a relative error of less than 10^{-5}. The convergence criteria for the end
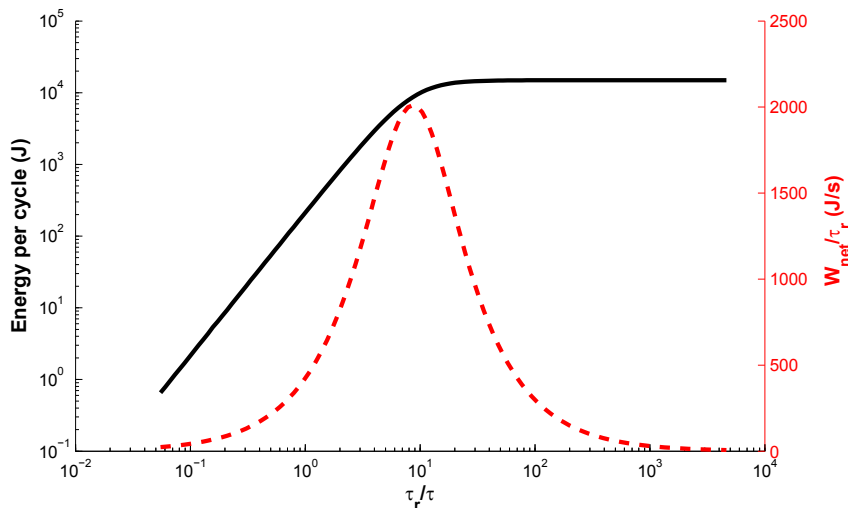
Fig. 11. The net work in the heat engine or the net heat in the heat pump (black solid line, left y-axis) and the net power or rate of net work (red dashed line, right y-axis) for different τ_r/τ. (For interpretation of the references to colour in this figure legend, the reader is referred to the web version of this article.)
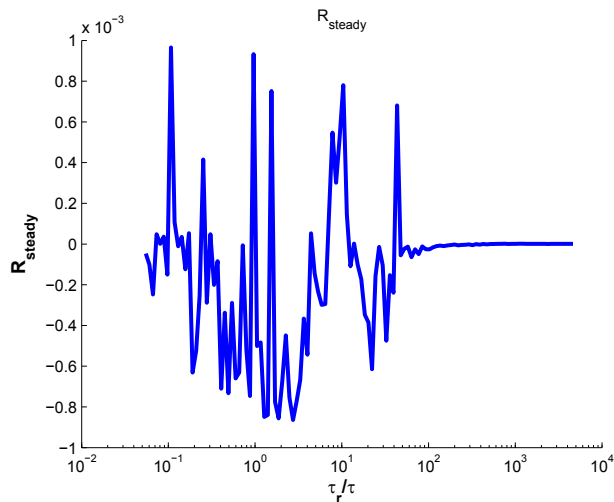
Fig. 12. Relative error in the steady cycle.

cycle, i.e., for steady state, is given by

$$R_{steady} = \left| \frac{Q_{net}^a - W_{net}^a}{Q_{net}^a} \right| \tag{76}$$

In the end-cycle, the two subsystems come to mutual equilibrium with the system energy conserved in each complete cycle, i.e. $Q_{net}^a = W_{net}^a$. The system is assumed to be in steady state when $R_{steady} < 10^{-3}$. This ratio is plotted in Fig. 12 for every data point in Figs. 10 and 11.

6. Conclusions

The SEAQT framework as demonstrated here and elsewhere is a first-principles, thermodynamic-ensemble based approach applicable to the entire nonequilibrium realm even that far-from-equilibrium. It furthermore provides a single kinematics and dynamics applicable across all temporal and spatial scales. Its application here to the modeling of a thermodynamic cycle is unlike that of traditional approaches based on equilibrium thermodynamics, which necessarily incorporate phenomenological efficiency parameters based on, for example, experiment to account for irreversibilities, or on so-called 'open quantum systems', which for a number of reasons are limited in their applicability.

Using the concepts of hypoequilibrium state and nonequilibrium intensive properties, the SEAQT framework is applied to a system with variable volume undergoing a cyclic process in which work is produced and energy in a heat interaction is exchanged with a series of reservoirs. The predictions made provide a clear description of the time evolution of the system from an initial transient cycle to an end-cycle, i.e., a steady cycle. As part of this description, intensive property evolutions of temperature, pressure, and volume on *P-T* and *P-V* diagrams are provided, which enhance one's general understanding of the system's nonequilibrium behavior at a thermodynamic level without the need for detailed fluid mechanics or heat transfer calculations. Such a nonequilibrium thermodynamic approach can be used as a first stage in the design process capturing the effects of irreversibilities and avoiding the need for costly experimental prototypes or detailed computational fluid dynamic calculations early on in the process.

Finally, the relative ratio of cycle period and relaxation time illustrates how strong the non-equilibrium effects are, and a case

study of optimizing the power output of the system relative to the non-equilibrium effects emphasizes the power of the SEAQT framework for design. In addition, since this framework is able to model the kinetics of a chemically reactive system, future work will make transient and steady cycle predictions of system behavior by replacing the heat reservoirs used in this study with a set of reaction mechanisms internal to the system.

Acknowledgments

References

[1] De Groot SR, Mazur P. Non-equilibrium thermodynamics. Courier Corporation; 2013.
[2] Zanchini E, Beretta GP. Recent progress in the definition of thermodynamic entropy. Entropy 2014;16:1547.
[3] Beretta GP, Gyftopoulos EP, Park JL, Hatsopoulos GN. Quantum thermodynamics. a new equation of motion for a single constituent of matter. Il Nuovo Cimento B Ser 1984;11(82):169–91.
[4] Beretta GP, Gyftopoulos EP, Park JL. Quantum thermodynamics. a new equation of motion for a general quantum system. Il Nuovo Cimento B Ser 1985;11(87):77–97.
[5] Beretta G. Nonlinear model dynamics for closed-system, constrained, maximal-entropy-generation relaxation by energy redistribution. Phys Rev E 2006;73:026113.
[6] Beretta GP. Maximum entropy production rate in quantum thermodynamics. J Phys Conf Ser 2010;237:012004.
[7] Beretta GP. Steepest entropy ascent model for far-nonequilibrium thermodynamics: unified implementation of the maximum entropy production principle. Phys Rev E 2014;90:042113.
[8] von Spakovsky M, Gemmer J. Some trends in quantum thermodynamics. Entropy 2014;16:3434–70.
[9] Li G, von Spakovsky MR. Steepest-entropy-ascent quantum thermodynamic modeling of the relaxation process of isolated chemically reactive systems using density of states and the concept of hypoequilibrium state. Phys Rev E 2016;93:012137.
[10] Li G, von Spakovsky MR. Generalized thermodynamic relations for a system experiencing heat and mass diffusion in the far-from-equilibrium realm based on steepest entropy ascent. Phys Rev E 2016. In publication, arXiv:1601.01344.
[11] Beretta GP, Al-Abbasi O, von Spakovsky MR. Steepest-entropy-ascent quantum thermodynamic framework for describing the non-equilibrium behavior of a chemically reactive system at an atomistic level. 2015. arXiv:1504.03994.
[12] Grmela M, Öttinger HC. Dynamics and thermodynamics of complex fluids. i. development of a general formalism. Phys Rev E 1997;56:6620–32.
[13] Öttinger HC, Grmela M. Dynamics and thermodynamics of complex fluids. ii. illustrations of a general formalism. Phys Rev E 1997;56:6633–55.
[14] Benzi R, Succi S, Vergassola M. The lattice boltzmann equation: theory and applications. Phys Rep 1992;222:145–97.
[15] Chen S, Doolen GD. Lattice boltzmann method for fluid flows. Annu Rev Fluid Mech 1998;30:329–64.
[16] Aidun CK, Clausen JR. Lattice-boltzmann method for complex flows. Annu Rev Fluid Mech 2010;42:439–72.
[17] Rapaport DC. The art of molecular dynamics simulation. Cambridge university press; 2004.
[18] Hoffmann KH. Quantum thermodynamics. Ann Phys 2001;10:79–88.
[19] Breuer H-P, Petruccione F. The theory of open quantum systems. Berlin: Oxford Univ. Press; 2002.
[20] Weiss U. Quantum dissipative systems. World Scientific; 1999.
[21] Gorini V, Kossakowski A, Sudarshan ECG. Completely positive dynamical semigroups of n-level systems. J Math Phys 1976;17:821–5.
[22] Lindblad G. On the generators of quantum dynamical semigroups. Commun Math Phys 1976;48:119–30.
[23] Gemmer J, Michel M, Mahler G. Quantum thermodynamics. Lecture notes in physics, vol. 784. Berlin: Springer Verlag; 2009.
[24] Levin GA, Jones WA, Walczak K, Yerkes KL. Energy transport in closed quantum systems. Phys Rev E 2012;85:031109.
[25] Panasyuk GY, Levin GA, Yerkes KL. Heat exchange mediated by a quantum system. Phys Rev E 2012;86:021116.
[26] Vogl P, Kubis T. The non-equilibrium greens function method: an introduction. J Comput Electron 2010;9:237–42.
[27] Keldysh LV. Diagram technique for nonequilibrium processes. Sov Phys JETP 1965;47:1515–27.
[28] Kadanoff LP, Baym G. Quantum statistical mechanics: Green's function methods in equilibrium and nonequilibrium problems. 1962. Benjamin New York.
[29] Rossani A, Kaniadakis G. A generalized quasi-classical boltzmann equation.

Phys A Stat Mech its Appl 2000;277:349–58.

[30] Garcia A, Wagner W. Direct simulation monte carlo method for the uehling-uhlenbeck-boltzmann equation. Phys Rev E 2003;68:056703.

[31] Torres-Rincon JM. Boltzmann-uehling-uhlenbeck equation. Springer; 2014. p. 33–45.

[32] Li G, Al-Abbasi O, von Spakovsky MR. Atomistic-level non-equilibrium model for chemically reactive systems based on steepest-entropy-ascent quantum thermodynamics. J Phys Conf Ser 2014;538:012013.

[33] Li G, von Spakovsky MR. Steepest-entropy-ascent quantum thermodynamic modeling of the far-from-equilibrium interactions between non-equilibrium systems of indistinguishable particle ensembles. 2016. arXiv:1601.02703.

[34] Cano-Andrade S, von Spakovsky MR, Beretta GP. Steepest-entropy-ascent quantum thermodynamic non-equilibrium modeling of decoherence of a composite system of two interacting spin-1/2 systems. In: ASME 2013 nternational mechanical engineering congress and exposition. American Society of Mechanical Engineers; 2013. V08BT09A043–V08BT09A043.

[35] Cano-Andrade S, Beretta GP, von Spakovsky MR. Non-equilibrium thermodynamic modeling of an atom-field state evolution with comparisons to published experimental data. In: Proceedings of the 12th joint european thermodynamics conference, Brescia, Italy; 2013. p. 1–5.

[36] Cano-Andrade S, Beretta GP, von Spakovsky MR. Steepest-entropy-ascent quantum thermodynamic modeling of decoherence in two different microscopic composite systems. Phys Rev A 2015;91:013848.

[37] Smith CE, von Spakovsky MR. Comparison of the non-equilibrium predictions of intrinsic quantum thermodynamics at the atomistic level with experimental evidence. J Phys Conf Ser 2012;380:012015.

[38] Martyushev LM, Seleznev VD. Maximum entropy production principle in physics, chemistry and biology. Phys Rep 2006;426:1–45.

[39] Gyftopoulos EP, Cubuk E. Entropy: thermodynamic definition and quantum expression. Phys Rev E 1997;55:3851–8.

[40] Gyftopoulos EP, Beretta GP. Thermodynamics: foundations and applications. Courier Corporation; 2005.

[41] Kosloff R. A quantum mechanical open system as a model of a heat engine. J Chem Phys 1984;80:1625.

[42] Levy A, Alicki R, Kosloff R. Quantum refrigerators and the third law of thermodynamics. Phys Rev E 2012;85:061126.

[43] Beretta GP. Quantum thermodynamic carnot and otto-like cycles for a two-level system. EPL Europhys Lett 2012;99:20005.

[44] Kosloff R. Quantum thermodynamics: a dynamical viewpoint. Entropy 2013;15:2100.

[45] Guggenheim E. Grand partition functions and so called "thermodynamic probability". J Chem Phys 1939;7:103–7.

[46] Hill TL. Statistical mechanics: principles and selected applications. Courier Corporation; 1956.

[47] Münster A. Zur theorie der generalisierten gesamtheiten. Mol Phys 1959;2:1–7.

[48] Brown WB. Constant pressure ensembles in statistical mechanics. Mol Phys 1958;1:68–82.

[49] Sack R. Pressure-dependent partition functions. Mol Phys 1959;2:8–22.

[50] Grmela M. Contact geometry of mesoscopic thermodynamics and dynamics. Entropy 2014;16:1652.

[51] Montefusco A, Consonni F, Beretta GP. Essential equivalence of the general equation for the nonequilibrium reversible-irreversible coupling (generic) and steepest-entropy-ascent models of dissipation for nonequilibrium thermodynamics. Phys Rev E 2015;91:042138.

[52] Beretta GP. Nonlinear quantum evolution equations to model irreversible adiabatic relaxation with maximal entropy production and other nonunitary processes. Rep Math Phys 2009;64:139–68.

[53] Corti DS. Isothermal-isobaric ensemble for small systems. Phys Rev E 2001;64:016128.

[54] Koper GJ, Reiss H. Length scale for the constant pressure ensemble: application to small systems and relation to einstein fluctuation theory. J Phys Chem 1996;100:422–32.

[55] Corti DS, Soto-Campos G. Deriving the isothermal–isobaric ensemble: the requirement of a shell molecule and applicability to small systems. J Chem Phys 1998;108:7959–66.

[56] Soto-Campos G, Corti DS, Reiss H. A small system grand ensemble method for the study of hard-particle systems. J Chem Phys 1998;108:2563–70.

[57] Li G, von Spakovsky MR. Application of steepest-entropy-ascent quantum thermodynamics to predicting heat and mass diffusion from the atomistic up to the macroscopic level. In: ASME 2015 international mechanical engineering congress and exposition. American Society of Mechanical Engineers; 2015. No. IMECE2015–53581.

[58] Al-Abbasi O. Modeling the non-equilibrium behavior of chemically reactive atomistic level systems using steepest-entropy-ascent quantum thermodynamics. Virginia Tech, Dept. of Mechanical Engineering; 2013. Ph.D. thesis, advisor: M. R. von Spakovsky.

[59] Smith C. Intrinsic quantum thermodynamics: application to hydrogen storage on a carbon nanotube and theoretical consideration of non-work interactions. Virginia Tech, Dept. of Mechanical Engineering; 2012. Ph.D. thesis, advisor: M. R. von Spakovsky.

[60] Attard P. On the density of volume states in the isobaric ensemble. J Chem Phys 1995;103:9884–5.

[61] Li G, von Spakovsky MR. Study of the transient behavior and microstructure degradation of a SOFC cathode using an oxygen reduction model based on steepest-entropy-ascent quantum thermodynamics. In: ASME 2015 international mechanical engineering congress and exposition. American Society of Mechanical Engineers; 2015. No. IMECE2015–53726.

[62] Bird RB, Stewart WE, Lightfoot EN. Transport phenomena. John Wiley & Sons; 2002.

Nomenclature

$(e^{i,a}, v^{i,a}, m^{i,a})$: macrostate properties in the ith subsystem of system A

(N,e,v,m): macrostate particle number, energy, volume, and magnetization of the system (N is omitted in general)

(p,q,s): microstate momenta, positions and spins of particles in the system

$\alpha_{a(b)}, \beta, \gamma$: intermediate parameters of the equation of motion in system A(B), defined by Eq. (24)

β^i: intensive properties corresponding to the energy in the ith subsystem

$\beta^{i,a}, \theta^{i,a}$: intensive properties in the ith subsystem of system A

β_r, γ_r: intensive properties of the reservoir

δx: dimension of system A

$\dot{W}_{net}$: net work rate

$\varepsilon_{heat\ pump}$: efficiency when the cycle acts as a heat pump

γ: state evolution trajectory in the Ginzburg-Landau equation

$\hat{\rho}$: density operator

$\hat{D}$: dissipation term in SEAQT equation of motion

$\hat{H}$: Hamiltonian

Λ^i: partition function in the ith subsystem and a function of (β^i, θ^i)

$\Lambda^{i,a}$: partition function of the ith subsystem of system A

Λ^{total}: partition function of system A

$\langle \cdot \rangle$: expectation value

$\langle \cdot \rangle^{a(b)}$: expectation value in system A(B)

$\langle \cdot \rangle^{i,a}$: expectation value in the ith subsystem of system A

$\mathscr{H}$: system thermodyanmic state space spanned by (e,v,m)

$\mathscr{H}_i$: ith subsystem in the thermodyanmic state space, composed of macrostates (e^i, v^i, m^i)

$\mathscr{K}$: system phase space spanned by (p,q,s)

$\mathscr{K}_i$: ith subsystem in phase space

Ω: density of states, numbers of microstates at a given macrostate (e,v,m)

ρ: probability distribution among microstates (in phase space), depending on the variables (p,q,s)

τ: relaxation time in the SEAQT equation of motion

τ_r: period of the cyclic process (reservoir)

θ^i: intensive properties corresponding to pressure in the ith subsystem

$\bar{\rho}$: probability distribution among macrostates, depending on the variables (e,v,m)

$\bar{\rho}^{i,a}$: probability distribution among macrostates in the ith subsystem of system A

$\bar{p}^i$: total probability in the ith subsystem

$\uparrow(\downarrow)$: superscript for the spin-up(down) subsystem of system A

^{quasi}: superscript stands for the quasi-equilibrium cycle

D_{self}: phenomenological self-diffusion coefficient

e: energy of the system in a macrostate

M: order of the hypoequilibrium state, i.e., the number of subsystems

m: magnetization of the system in a macrostate

P^i: pressure of the ith subsystem

$p_{x,i}$: momentum of the ith particle in the x direction for a microstate

Q: canonical ensemble partition function for a system containing N particles in a volume v at temperature T

$Q_{upper/lower}$: heat integral of the upper/lower half of the cycle on the T-S diagram

$q_{x,i}$: position of the ith particle in the x direction for a microstate

R_{steady}: relative error in determining the steady cycle

s_i: spin of ith particle in the x direction for a microstate

T^i: temperature of the ith subsystem

v: volume of the system in a macrostate

W_{net}, Q_{net}: net work and heat in one complete cycle

$W_{upper/lower}$: work integral of the upper/lower half of the cycle on the P-$\mathbf{V}$ diagram

X_γ^H: reversible term in the Ginzburg-Landau equation

Y_γ^H: reversible term in the Ginzburg-Landau equation